RESEARCH ARTICLE

SAMRIDDHI Volume 13, Special Issue 2, 2021 Print ISSN : 2229-7111 Online ISSN : 2454-5767

Twin Boundary in Pure and Strontium Doped Barium Titanate

Devidas Gulwade

Deptt. of Physics, Vivekanand Education Society's College of Arts, Science and Commerce, Sindhi Society, Chembur, Mumbai-71, India; e-mail: devidas.gulwade@ves.ac.in

ABSTRACT

In the present investigation, microstructures of pure and strontium doped BaTiO3 were studied using electron back scattered diffraction (EBSD). The compositions were synthesized by using solid state reaction. The presence of single phase was confirmed using X-ray diffraction. Further, synthesized compounds were sintered using two routes, namely, conventional sintering and microwave sintering. Microstructures studied by electron backscattered diffraction revealed the formation of 3 twin boundaries, for both conventional and microwave sintered samples. The fraction of coherent twin boundaries in conventionally sintered BaTiO3 was higher than that in the microwave sintered BaTiO3. Also, the fraction of twin boundaries decreased with increase in strontium dopant concentration for conventionally sintered samples.

Keywords: Barium titanate, Ferroelectric properties, Grain boundary, Perovskites, twinning.

SAMRIDDHI : A Journal of Physical Sciences, Engineering and Technology, (2021); DOI : 10.18090/samriddhi.v13spli02.25

INTRODUCTION

Doped barium titanate ($BaTiO_3$) is an attractive material for various microelectronic applications. The most widely investigated dopants are Sn [1],[2] Sr[3], La[4]-[6], Zr [7]-[8] Ce [9]-[13] and Y[14]-[15]. The dielectric properties of ferroelectric materials depend on both the crystal structure as well as the microstructures. The microstructures can be altered by using various synthesis and processing routes. The effect of grain size on ferroelectric properties has been widely studied, but there are contradictory opinions on how it may influence the nature of transition and dielectric constant [16]-[20]. Further, to correlate microstructures and properties, variation of grain boundary distribution and its effect on properties as a function of processing conditions must be established. A control of grain boundary characteristics with optimum processing may lead to precise control of microstructure and consequently its properties [21]. Recently, the effect of grain boundary distribution, especially $\Sigma 3$ grain boundary on the domain structure, anomalous grain growth and ferroelectric properties was studied. The $\Sigma 3$ twin boundary is also observed in other perovskite materials like lead zirconate and strontium titanate [22]. In $BaTiO_3$, $\Sigma 3$ grain boundary has been correlated with hexagonal $BaTiO_3$ ordering, Ti non-stoichiometry and anomalous grain growth. The effect of the grain boundary characteristics on the positive temperature coefficient (PTC) of resistance was examined and it was shown that $\Sigma 3$ special boundary was PTC inactive and its fraction needs to be minimized. The percentage of these special grain boundaries was reported to remain constant with change in sintering time and also not to be affected significantly by grain growth.[23]-[24] The {111} twins that cause abnormal grain growth, form around the second phase - $Ba_6Ti_{17}O_{40.}$ [25]. The $BaTiO_3$ seed grains with double twins were observed to grow to a very large size, resulting in secondary anomalous grain growth (SAGG). SAGG has been explained in terms of favorable nucleation at the reentrant edges formed by the double twins [26]. Two-dimensional nucleation

Corresponding Author : Devidas Gulwade, Deptt. of Physics, Vivekanand Education Society's College of Arts, Science and Commerce, Sindhi Society, Chembur, Mumbai-71, India; e-mail: devidas.gulwade@ves.ac.in

How to cite this article : Gulwade, D. (2021). Twin Boundary in Pure and Strontium Doped Barium Titanate.

SAMRIDDHI : A Journal of Physical Sciences, Engineering and Technology, Volume 13, Special Issue (2), 261-267

Source of support : Nil

Conflict of interest : None

on a twin-plane reentrant edge facilitates the grain growth in the absence of liquid phase as a result of higher nucleation rate as compared to a flat surface [27]. At sintering temperature, the grains possessing a double twin were observed to exhibit anomalous grain growth [28]. Further, the faceted twin boundaries are believed to result in anomalous grain growth (AGG). A titanium rich $BaTiO_3$ exhibits anomalous grain growth and this has been correlated with the presence of second phase [29]. Normal grain growth (NGG) occurs with excess barium, whereas AGG with equiaxial grain occurs with excess titanium between 0 and 0.3 at.%. The double twin assisted AGG has been reported to occurs with excess titanium >0.3 at.%.[30]. The AGG occurs when the grain boundaries are singular with faceted hill-and-valley or flat shapes. Similar work based on Sr doped $BaTiO_3$, in Ti excess region has established the presence of {111} twin formation which is in line with the formation of second phase assisted twin growth observed in pure $BaTiO_3$ [31].

In order to correlate and predict dependence of property on the grain boundary distribution, the effect of dopants on the grain boundaries and properties needs to be studied thoroughly and this has been the motivation for the present investigation. Microstructure in metals is widely studies using electron back scattered diffraction (EBSD). In this investigation, we have studied microstructure using EBSD. In this work, we report preparation of sintered ceramic materials for study of microstructure using EBSD. Furthermore, we report analysis of the grain boundary distribution in pure $BaTiO_3$ (BT) and Strontium doped $BaTiO_3$ (BST) sintered using two different techniques (conventional and microwave).

EXPERIMENTAL

The compositions corresponding to $Ba_{1-x}Sr_xTiO_3$ (x = 0, 0.1, 0.2, 0.25) were prepared by using conventional solid-state reaction. The starting materials, $BaCO_3$, $SrCO_3$ and TiO_2 were procured from Aldrich Chemicals. Stoichiometric amounts of the starting materials were mixed in a ball-mill with zirconia as a grinding media in ethanol. The powder was calcined at 1100 ^oC for 12 h, followed by repetitive stages of ball milling and calcinations. The powder was characterized by X-Ray diffraction (XRD) using Cu Ka radiation and slow scan rate (0.01^o/10s) at room temperature to confirm the perovskite phase. The lattice parameters were extracted from the diffraction patterns by indexing the data using the tetragonal space group P4/mmm with FULLPROF software [32]. The powder was ball-milled for 24 h in a Teflon jar using partially stabilized zirconia as a milling media in ethyl alcohol. Further, the resultant powder was dried, pelletized using tungsten carbide die and sintered at 1350^{o}C by two different techniques, namely, conventional sintering and microwave sintering. Conventionally sintered samples were heated at 5^{o}C/minute for two different time duration; 1 hour and 4 hours labeled as CS1h and CS4h respectively. For the microwave sintered samples, the first (MW1) was heated at 5 ^{o}C/minute, identical to the heating rate for CS1h and CS4h, while the other (MW2) was heated at a faster rate of 20^{o}C/minute. The dielectric measurements were done in the temperature range between ambient and 300^{o}C at different frequencies using a HP impedance analyzer (4192A). A flat face of sintered cylindrical pellet was polished using SiC abrasive papers, successively using finer abrasive papers. Further, final polishing is carried out using colloidal silica using polishing cloth mounted on a rotating wheel. The microstructures were studied by electron backscattered diffraction (EBSD) with a commercial TexSem Laboratories Ltd., USA (TSL) system attached to a FEI Quanta 200 HV scanning electron microscope (SEM). The EBSD data was acquired on a polished flat face of a cylindrically sintered pellet. The EBSD patterns were indexed using cubic space group symmetry, since the tetragonality was less than 1% for all compositions studied in the present investigation.

RESULTS AND DISCUSSIONS

XRD and Dielectric Characterization

The XRD patterns for all calcined compositions are shown in Figure 1(a). The XRD patterns showed that all the compositions exhibited a single phase. The secondary phases namely $Ba_6Ti_{17}O_{40}$ and $Ba_4Ti_{13}O_{30}$ are usually observed in pure $BaTiO_3$, exhibit high intensity peaks between 20^o to 35^o 2q [JCPDF file number 01-083-1875]. The expanded view of XRD patterns (2q between 20^o to 35^o) is shown in Fig 1(b) for all the compositions. Fig 1 confirms the formation of perovskite phase and absence of any other secondary phases that are believed to be related with formation of twin boundaries. The tetragonality decreased with an increase in Sr dopant concentration, which is in good agreement with the corresponding change in Goldsmith tolerance factor (see Figure 1(c)). The dielectric

constant for all compositions as a function of temperature is plotted in Figure 2. No variation in the dielectric properties between conventionally sintered and Microwave sintered $BaTiO_3$ was observed in the present study. The transition temperature decreased and the diffuseness of the phase transition increased with the increase in strontium dopant concentration. The change in dielectric properties as a function of strontium dopant concentration is in agreement with that reported in the literature [33].

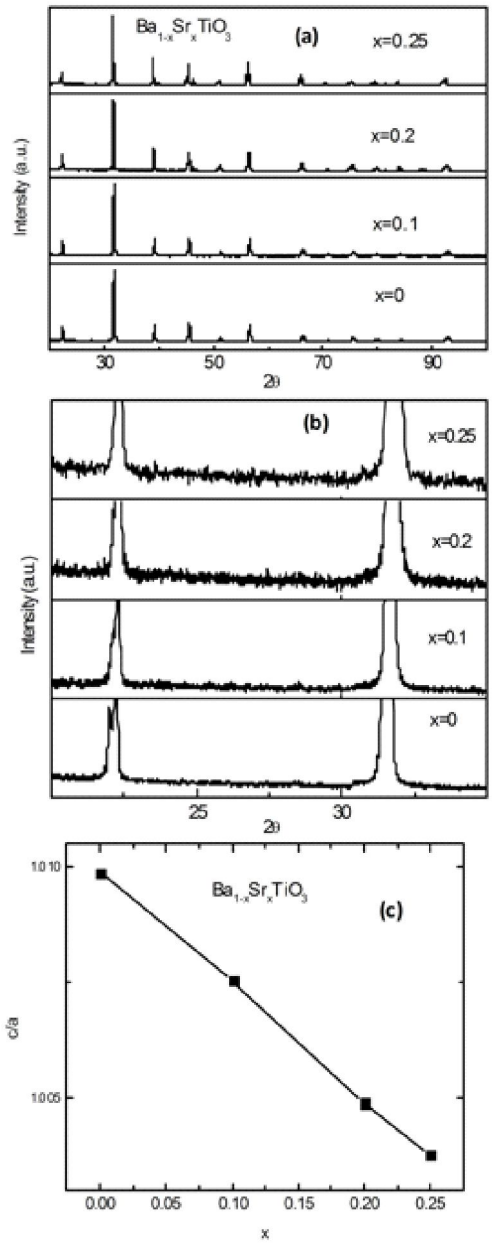

Figure 1: XRD pattern for $Ba_{1-x}Sr_xTiO_3$ compositions (a); extrapolated in between 20 and 35 °(b); tetragonality as a function of dopant concentration (c).

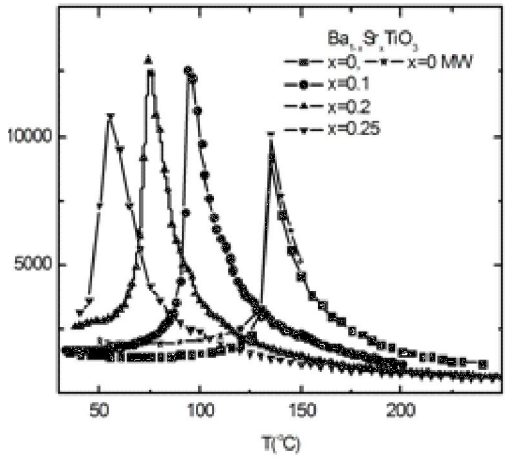

Figure 2: Dielectric constant as a function of temperature for $Ba_{1-x}Sr_xTiO_3$

Microstructures of pure $BaTiO_3$ and BST

The image quality map for solid state sintered (CS4h) $BaTiO_3$ is shown in Figure 3. Few twin boundaries are highlighted with arrow. The conventionally sintered (CS4h) $BaTiO_3$ exhibited ~ 100 μm sized grains, with few anomalously grown grains [34]. The grain misorientation distribution was compared with the random Mackenzie distribution [35]. From the grain boundary misorientation distribution, it was observed that Barium titanate exhibits a peak at 60° misorientation as compared to random distribution (Mackenzie). This is indicative of a preferred grain boundary type. The coincident site lattice (CSL) model defines a grain boundary using a fraction of atoms in the grain boundary plane which are coincident to both lattices sharing the grain boundary. The Σ value denotes the fraction of atoms in coincidence, for e.g. Σ3 boundary has 1 in 3 atoms in coincidence. The Σ3 boundary is 60°<111> (misorientation-axis pair) twin boundary. In practice, the CSL grain boundary deviates from ideal CSL orientation. Therefore, in the present investigation, special grain boundary exhibiting deviation less than K/Σ^n was considered as CSL boundary. In the Brandon criterion, 15° for K and ½ for n is generally used; this is considered as a broad criterion of classification [36]. Therefore, the allowed deviation from exact CSL is 8.66° for Σ3 grain boundary. The percentage of Σ3 grain boundary in conventionally sintered composition was ~12 % and a large fraction of Σ3 grain boundary exhibited deviation less than 1°. Further, the twin boundaries

and coherent twins were calculated using reconstructed boundaries using TSL software. In addition to the misorientation (angle/axis) criterion, the boundary plane {111} must coincide with the twinning plane. However, complete information is not available in two dimensional EBSD scans and serial sectioning or three dimensional sampling techniques are required to confirm whether the boundary is really coherent. By examining the three dimensional characters of many twin boundaries, Randle et al.[37] established that when the traces are aligned, the boundary and twinning planes were also aligned. Therefore, the coherent twin fraction was calculated on the basis of alignment between the trace of boundary plane and twining plane using the TSL software [38]. The Σ3 twin boundary and coherent twin fraction is provided in Table-1. The twin fraction for CS1h and CS4h was almost in agreement with each other and exhibited similar values (see Table-1 and 2). The minor difference between the Σ3 twin boundary and coherent twin fraction is due to the difference in the grain size of the two samples. The CS1h has an average grain size of 66 μm, while the CS4h has an average grain size of 120 μm.

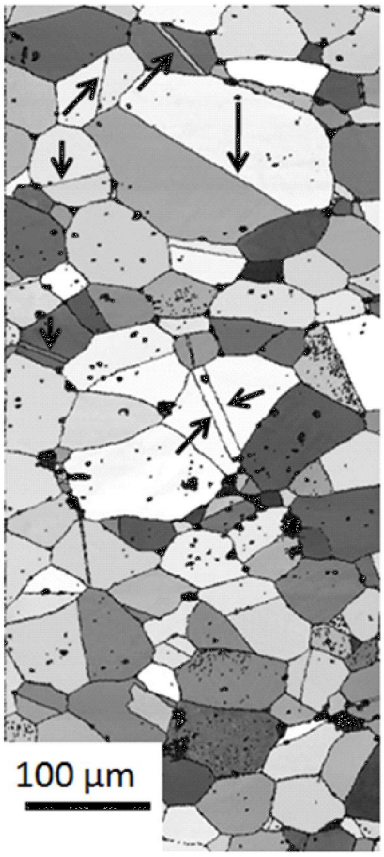

Figure3: Microstructure of sintered $BaTiO_3$

The average grain size and fraction of special grain boundary is given in Table-1. The fraction of coherent twins in MW1 and MW2 were less relative to those for CS samples. The MW2 sintered samples with a higher heating rate exhibited a finer grain size relative to that for CS or MW1(heating rate same as that of CS). The grain growth was suppressed due to higher heating rate and is a well observed sintering phenomenon [39]. The fraction of low angle grain boundaries in CS1h (0.05) was less relative to that for the microwave sintered BT (0.02). Also, the fraction of CSL boundaries in CS was 0.21, whereas it was 0.17 for the MW processed sample (see Table-2). In other words, the density of low angle and CSL special low energy grain boundary was less in MW processed sample. The decrease in grain size in MW was followed by a decrease in twin fraction of CSL boundary, in comparison to the conventionally processed sample. Additionally, microwave sintered BT did not showed anomalously grown grains, unlike conventionally sintered BT samples. This lack of exaggerated grain growth is in agreement with lower fractions of twin boundary. Further, the OIM scans were divided in two parts namely, grains exhibiting twin and grains without twins. Figure 4 shows that the grain size distribution for grains with and without twins is similar. However, grains exhibiting twins displayed a higher average grain size. The twin length and corresponding grain size diameter is plotted in Figure 5. The grain size increased with an increase in length of twin boundary implying that growth of twin boundary resulted in grain growth. Aspect ratio (ratio of length of minor axis to major axis) was also calculated by fitting grains with ellipse using TSL software. The aspect ratio for grains with and without twin boundary is plotted in Figure 6. Aspect ratio distribution between grains with and without twins was almost similar. The aspect ratio of majority of grains exhibiting twins was more than 0.5 i.e. implying equiaxial grains. The microstructure of conventionally sintered BST compositions at 1350°C for 4 h was also studied. The average grain size for all BST compositions is provided in Table-2. Barium titanate exhibited abnormally large grains which were not observed in BST compositions. The grain size decreased with increase in Sr dopant concentration, this corroborates with reported literature [40]. The percentage of CSL grain boundary decreased with an increase in the strontium concentration. The fraction of Σ3 grain boundary was maximum amongst all other CSL boundaries. Also,

deviation of the Σ3 grain boundary was similar to that observed for pure $BaTiO_3$; large fraction exhibited deviation below 1°. The Σ3 grain boundary was related with grain growth and/or anomalous grain growth. The higher Sr doped compositions ($Ba_{1-x}Sr_xTiO_3$, x=0.2 and 0.25) does not exhibited exaggerated grain growth, unlike pure $BaTiO_3$, which is in agreement with lower percentage of Σ3 grain boundary.

Table-1: The fraction of Σ3, coherent twin boundary and average grain size for Conventionally sintered (CS) and Microwave sintered (MW1 and MW2) $BaTiO_3$

$BaTiO_3$	Σ3	Coherent Σ3 fraction	Avg. Grain size (μm)
CS 1h	0.16	0.06	66
MW1	0.09	0.01	40
MW2	0.11	0.02	37

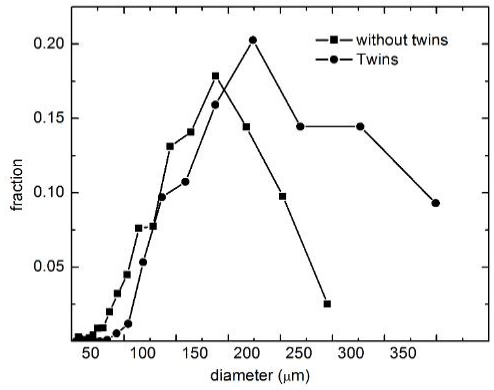

Figure 4: Grain size distribution in twined and non-twined grains in conventionally sintered $BaTiO_3$

Table-2: The fraction of Σ3, coherent twin boundary and average grain size for $Ba_{1-x}Sr_xTiO_3$ compositions, conventionally sintered at 1350 °C for 4h.

$Ba_{1-x}Sr_xTiO_3$	Σ 3	Coherent Σ3 fraction	Avg. Grain size (μm)
CS 4h (BT; x=0)	0.14	0.04	120
x=0.1	0.09	0.01	112
x=0.2	0.03	-	45
x=0.25	0.03	0.005	33

Two different types of twins (growth and deformation) are reported in barium titanate. Both growth and deformation twins occur in the tetragonal modification. Growth twins (with {111} twinning plane) are formed in cubic phase during grain growth at high temperatures and preserved in tetragonal barium titanate. Deformation twins occur as a result of cubic-tetragonal phase transition. The twins observed in the present case are growth twins. The sintering conditions play a very important role in formation of {111} twins. This is also clear from the present investigation - conventionally sintered samples resulted in more S3 boundaries as compared to microwave sintered sample. An important factor influencing twining percentage is the strain present in the sample. Change in lattice parameter causes a considerable strain within the grains which may result in the formation of twins. With the increase in dopant concentration, the tetragonality decreases, resulting in less fraction of twinning.

Effect of Twinning on Grain Size Distribution

EBSD scan recorded is divided into two parts, namely grains exhibiting twins and grains that do not depict twin boundary. The grain size distribution for grains exhibiting twins and not exhibiting twins was similar with a difference that twinned grains exhibited few grains of higher sizes. Further, higher grain size increased the probability of twin formation. The aspect ratio between twinned and non twinned grains also resembled with each other; grain exhibiting twins were equiaxed. (cf. Figure 4, 5 and 6) The bulk texture or the texture index does not show any trend, which indicates that the twinning phenomenon is more sensitive to growth conditions rather than the initial texture of the material. The total scan exhibits weaker texture as this is a mixture of strongly textured twins as well weakly textured non-twinned partitions. This work establishes preference in the orientations leading to 60°<111> i.e. Σ3 twin boundary. The conventionally sintered sample (CS1h and CS4h) showed higher fraction of Σ3 boundaries as compared to microwave sintered samples. This could possibly be due to the difference in the grain size distribution between the two methods. The conventionally sintered samples has anomalous grain growth, while the microwave sintered samples and strontium doped samples has uniform grain size distribution.

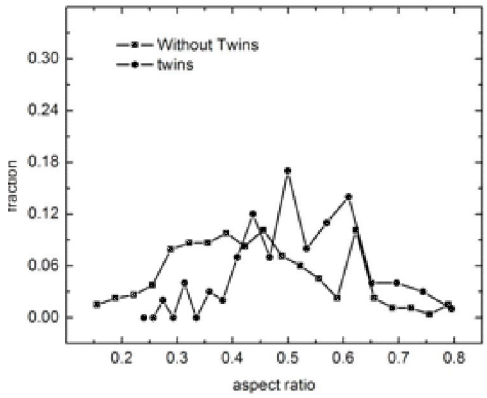

Figure 5: Grain size diameter as a function of twin length

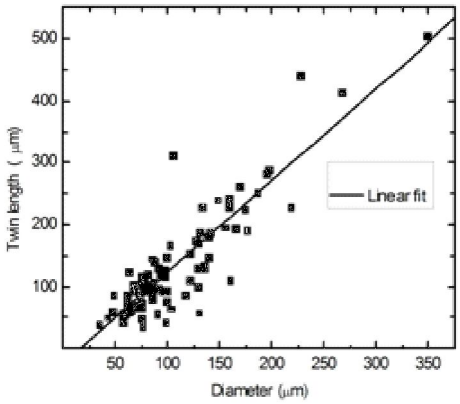

Figure 6: Aspect ratio in twined and non-twined grains in $BaTiO_3$

CONCLUSIONS

We have examined grain boundary characteristics of pure $BaTiO_3$ and Strontium doped $BaTiO_3$. Microwave sintered $BaTiO_3$ exhibited a lower fraction of twin boundary and normal grain growth unlike conventionally sintered $BaTiO_3$ which showed anomalous growth. In BST, twin fraction and the grain size decreased with increase in the strontium concentration. The present work clearly establishes that twin boundaries grow in the absence of parasite phase in pure and doped $BaTiO_3$. The work establishes a growth in grain size followed by increased length of twin boundary. Also, grain size distribution and aspect ratio between twinned and non-twinned grains has been probed. Further, a study exhibiting wide variation in microstructure may lead to more interesting observations.

ACKNOWLEDGMENT

The author thanks to Prof. I. Samjdar, Prof. P. Gopalan and Prof. R. Khatirkar for discussions during course of this work.

REFERENCES

[1] R. Vivekanandan, and T. R. N. Kutty, "Hydrothermal synthesis of $Ba(Ti,Sn)O_3$ fine powders and dielectric properties of the corresponding ceramics," Ceram. Int., vol.14, pp. 207-216, 1988.

[2] V.V. Shvartsman, and W. Kleemann, J. Dec, Z. K. Xu and S. G. Lu, "Diffuse phase transition in $BaTi_{1-x}Sn_xO_3$ceramics: An intermediate state between ferroelectric and relaxor behavior" J. Appl. Phys., vol. 99, pp. 124111, 2006.

[3] Y..Bao, B. Huang, K.Zhou, J.Roscow, E.Roake, M. Hopkins, D.Zhang, Y. Zhang, C. Bowen, "Hierarchically structured lead-free barium strontium titanate for low-grade thermal energy harvesting," Ceramics International, vol. 47, pp. 18761-18772, 2021; Y. Zhai, X. Xie, R. Zhou,X. Li,X. Liu, and S. Liu, "High performance room temperature ferroelectric barium strontium titanate ceramics by spark-plasma-sintering ultrafine nanocrystals," Ceramics International, vol 45, pp. 15526-15531, 2019; B. S. Chiou, and J. W. Liou, "Dielectric characteristics of doped $Ba_{1-x}Sr_xTi0_3$ at the paraelectric state, " Mater. Chem. Phys., vol. 51, pp. 59-63, 1997;

[4] F.D. Morrison, D.C. Sinclair, and A. R. West, "Electrical and structural characteristics of lanthanum-doped barium titanate ceramics," J. Appl. Phys., vol. 86, pp. 6355-6366, 1999.

[5] F.D. Morrison, D.C. Sinclair, J.M.S. Skakle, and A.R. West, "Novel Doping Mechanism for Very-High-Permittivity Barium Titanate Ceramics," J. Am. Ceram. Soc., vol.81**,** pp. 1957-1960, 1998.

[6] F.D. Morrison, D.C. Sinclair, and A.R. West, "An Alternative Explanation for the Origin of the Resistivity Anomaly in La-Doped $BaTiO_3$," J. Am. Ceram. Soc., vol.84, pp.474-476, 2001.

[7] B. Jaffe, W.R. Cook, and H. Jaffe, "Piezoelectric Ceramics," Academic Press Inc. London, 1971.

[8] D. Hennings, A. Schnell, and G. Simon, "Diffuse Ferroelectric Phase Transitions in $Ba(Ti_{1-y}Zr_y)0_3$ Ceramics, " J. Am. Ceram. Soc., vol. 65, pp.539-544, (1982).

[9] D. Makovec, and D. Kolar," Internal Oxidation of Ce^{3+}–$BaTiO_3$ Solid Solutions, " J. Am. Ceram. Soc., vol.80 , pp.45-52, 1997.

[10] D. F. K. Hennings, B. Schreinemacher, and H. Schreinemacher, "High-permittivity dielectric ceramics with high endurance," J. Euro. Ceram. Soc., vol. 13, pp. 81-88, 1994.

[11] A.Chen, Y.Zhi, J.Zhi, P.M.Vilarinho, and J.L. Baptista, "Synthesis and Characterization of $Ba(Ti_{1-x}Ce_x)O_3$ Ceramics," J. Euro. Ceram. Soc., vol.17, pp. 1217-1221, 1997.

[12] A. Chen, J. Zhi, and Y. Zhi, "Ferroelectric relaxor $Ba(Ti,Ce)O_3$," J. Phys.: Condens. Matter, vol. 14, pp. 8901-8912, 2002.

[13] Z. Yu, C. Ang, Z. Jing, and P.M. Viarinho, J. L. Baptista, "Dielectric properties of from 10^2 to 10^5 Hz in the temperature range 85 - 700 K," J. Phys.: Condens. Matter, vol.9, pp. 3081-3088, 1997.

[14] Z. Jing, C. Ang, Z. Yu, P. M. Vilainho, and J. L. Batptista, "Dielectric properties of Ba(Ti1"yYy)O3 ceramics" J. Appl. Phys., vol. 84, pp.983-986, July 1998.

[15] J. Zhi, A. Chen, Y. Zhi, P. M. Vilainho, and J. L. Batptista, "Incorporation of Yttrium in Barium Titanate Ceramics," J. Am. Ceram. Soc., vol.82, pp.1345-1348, 1999.

[16] G. Arlt, D. Hennings, and G. D. With, "Dielectric properties of fine-grained barium titanate ceramics," J. Appl. Phys. vol.58, pp.1619-1625, 1985.

[17] H.T. Martirena, and J.C. Burfoot, "Grain-size effects on properties of some ferroelectric ceramics," J. Phys. C: Solid state Phys. vol.7, pp.3182-3192, 1974.

[18] W.R. Buessem, L.E.Cross, and A.K.Goswami, "Phenomenological Theory of High Permittivity in Fine-Grained Barium Titanate," J. Am. Ceram. Soc., vol.49, pp.33-36, 1966. ; W.R. Buessem, L.E.Cross, and A.K. Goswami, "Effect of Two-Dimensional Pressure on the Permittivity of Fine- and Coarse-Grained Barium Titanate, " J. Am. Ceram. Soc. vol.49, pp.36-39, 1966.

[19] K. Uchino, E. Sadananga, and T. Hirose, "Dependence of the Crystal Structure on Particle Size in Barium Titanate," J. Am. Ceram. Soc., vol.72, pp.1555-1558, 1989.

[20] V. Buscaglia, M.T. Buscaglia, M. Viviani, L. Mitoseriu, P. Nanni, V. Trefiletti, P. Piaggio, I. Gregora, T. Ostapchuk, J. Pokorny, and J. Petzelt, "Grain size and grain boundary-related effects on the properties of nanocrystalline barium titanate ceramics," J. Eur. Ceram. Soc., vol.26**,** pp.2889-2898 (2006).

[21] S.Y. Choi, and S.J. L. Kang, "Sintering kinetics by structural transition at grain boundaries in barium titanate," Acta Mater. vol.52, pp. 2937-2943, 2004.

[22] F. Ernst, M.L. Mulvihill, O. Kienzel, and M. Ruhle, "Preferred Grain Orientation Relationships in Sintered Perovskite Ceramics," J. Am. Ceram. Soc. vol.84, pp.1885-1890, 2001.

[23] J. Seaton, and C. Leach, "Evolution of low sigma grain boundaries in PTC thermistors during sintering," J. Euro. Ceram. Soc., vol.25, pp.3055-3058, 2005.

[24] J. Seaton, and C. Leach, "Formation and retention of low R interfaces in PTC thermistors," Acta. Mater. vol.53**,** pp.2751-2758, 2005.

[25] B.K. Lee, S.J. L. Kang, "Second-phase assisted formation of {111} twin in Barium titanate,"Acta Mater, vol.49**,** pp.1373-1381, 2001.

[26] M.G. Kang, D.Y. Kim, H.Y. Lee, and N. M. Hwang, "Temperature Dependence of the Coarsening Behavior of Barium Titanate Grains," J. Am. Ceram. Soc. vol.83, pp.3202-3204, 2000.

[27] H. Schmelz, and A. Meyer, "Control of {111} twin formation and abnormal grain growth in $BaTiO_3$," Ceram. Forum Int., vol.59, pp.436-440, 1982.

[28] H.Y. Lee, J.S. Kim, and D.Y. Kim, "Effect of Twin-Plane Reentrant Edge on the Coarsening Behavior of Barium Titanate Grains," J. Am. Ceram. Soc., vol.85, pp. 977-980, 2002.

[29] 29. S. B. Lee, W. Sigle, and M. Ruhle, "Investigation of grain boundaries in abnormal grain growth structure of TiO2-excess BaTiO3 by TEM and EELS analysis.," Acta Mater., vol.50 pp.2151-2162 (2002).

[30] Y.K. Cho, S.J. L. Kang, and D. Y. Yoon, "Dependence of Grain Growth and Grain-Boundary Structure on the Ba/Ti Ratio in $BaTiO_3$," J. Am. Ceram. Soc. vol.87, pp.119-124, 2004.

[31] B.K. Lee,Y. I. Jung,S.J. L. Kang, and J. Nowotny, "{111} Twin Formation and Abnormal Grain Growth in Barium Strontium Titanate," J. Am. Ceram. Soc. vol.86**,** pp.155-160, 2003.

[32] J.R. Carvajal, "FULLPROF" Version 2 K, Laboratoire Leon Brillouin CEA CNRS (2000)

[33] A.D. Hilton, and B.W. Ricketts, "Dielectric properties of $Ba_{1"x}Sr_xTiO_3$ ceramics," J. Phys. D: Appl. Phys., vol.29, pp.1321-1325, 1996.

[34] A. Koblischka-Veneva, and F Mücklich, "Orientation imaging microscopy applied to $BaTiO_3$ ceramics," Crystal Engineering. vol.5 , pp.235-242, 2002.

[35] V. Randle, "Relationship between coincidence site lattice, boundary plane indices, and boundary energy in nickel," Mater. Sci. Technol. Vol.15, pp.246-252, 1999.

[36] D. G. Brandon, "The structure of high-angle grain boundaries," Acta Metall., vol.14**,** pp.1479-1484, 1966.

[37] V. Randle, "Special boundaries and grain boundary plane engineering," Scripta Mat. vol.54, pp.1011-1015, 2006.

[38] TSL OIM analysis software version 5.3

[39] S. Mahajan, O. P. Thakur, D. K. Bhattacharya, and K. Sreenivas, "Study of Structural and Electrical Properties of Conventional Furnace and Microwave-Sintered $BaZr_{0.10}Ti_{0.9}0O_3$ Ceramics," J. Am. Ceram. Soc. vol.92**,** pp.416-423, 2009.

[40] J. H. Jeon, "Effect of $SrTiO_3$ concentration and sintering temperature on microstructure and dielectric constant of $Ba_{1-x}Sr_xTiO_3$," J. Euro. Ceram. Soc.,vol.24**,** pp.1045-1048, 2004.